On the Coupling Between a Quasiperiodic Structure and an Asymmetric Output Arm

Levi Schächter and John A. Nation

Abstract—**We present the analysis of the electromagnetic coupling between a quasi-periodic disk loaded structure and an asymmetric radial arm. The field is excited by a current distribution which models the spatial growth of a space-charge wave in a traveling wave structure. The output power is controlled by a stub tuner. Maximum power does not occur for minimum reflection. The condition for this regime is presented.**

I. Introduction

In many high power devices the electromagnetic energy is confined and guided by metallic surfaces. These surfaces play an important role in the interaction process of the electrons with the electromagnetic wave(s). A klystron, for example, consists of a metallic pipe to which two or more cavities are connected. The pipe is designed such that at the frequency of interest the electromagnetic wave is below cutoff and in the absence of the beam the cavities are *isolated*. In this kind of structure power levels of 50 MW at 11.4 GHz were achieved at SLAC [1] but since the interaction occurs in the close vicinity of the cavity gap the gradients at the output cavity are high and the system is susceptible to RF breakdown.

This problem is less severe in a disk loaded traveling wave tube (TWT) which consists of a series of *coupled* cavities. These cavities are basically a short section of a periodic structure. In this case the interaction is no longer confined to the vicinity of the cavity, but it is distributed along the entire structure. The first experiments on high power TWT performed at Cornell [2] indicated that 100 MW at 8.76 GHz can be achieved before the system oscillates. Although no RF breakdown was observed in these kind of structures the fact that the input is no longer isolated from the output allows waves to be reflected backwards and this feedback may ultimately cause the system to oscillate. To envision the process imagine that 20 kW of power are injected into the system and the one-pass gain is 40 dB. Thus, before the RF leaves the system 200 MW of power are available. If the reflection coefficient at the output is $\rho = 0.1$ and a similar reflection occurs at the input end then the contribution of the reflection is of the same order as the injected power and the system oscillates.

Manuscript received November 23, 1993; revised March 9, 1994. This work was supported by the Binational United States-Israel Science Foundation and by the United States Department of Energy.

L. Schächter is the with Department of Electrical and Computer Engineering, Ben-Gurion University, Beer Sheva 84105, Israel.

J. A. Nation is with the Laboratory of Plasma Studies and School of Electrical Engineering, Cornell University, Ithaca, NY 14853 USA.

IEEE Log Number 9406819.

In order to isolate the input from the output the TWT was split in two sections separated by a sever (lossy material whose radius is below cut-off). The second set of experiments on two stage high power TWT indicated that power levels in excess of 400 MW are achievable with no indication of RF breakdown [3]. In this case however the output spectrum was 300 MHz wide and a significant amount of power (up to 50%) was measured in asymmetric sidebands. The latter observation was investigated theoretically [4] and it was concluded that it is a result of amplified noise at frequencies selected by the interference of the two waves bouncing between the ends of the last stage. In fact it has been shown [5] that what we call amplifier and oscillator are the two extreme of possible regimes of operation and any practical device operates somewhere in between according to the degree of control of the reflection process. We have suggested [6] a method to eliminate the problem of reflections by designing a structure in which the time it takes the first reflection to reach the input end is of the same order of magnitude as the electron pulse length. Thus, by the time the reflection becomes relevant there are no more electrons to interact with. This method was successfully demonstrated [7] experimentally and power levels of 200 MW were achieved at 9 GHz. The spectrum of the output signal was less than 50 MHz and the pass-band of the periodic structure was less than 200 MHz. For this reason we call it a narrow band structure (NBS). The inner pipe of this structure has a radius of 6.2 mm and the exponential decay (of the first evanescent wave) between two cavities is of the order of 0.1. This low coupling level resembles the isolation of the cavities in a klystron. Furthermore the low energy (group) velocity is directly associated with an increased spatial growth rate which, in terms of dB/cm, can be 5–6 times larger than in a regular TWT and about half to a third of the output cavity of an klystron (taking the effective aperture as the interaction length). The 200 MW power levels generated with the NBS were accompanied by gradients larger than 200 MV/m. Although no RF breakdown was experienced, for any further increase in the power levels it will be necessary to increase the volume of the last two or three cells in order to minimize the electric field on the metallic surface. Thus, the system becomes quasi-periodic.

To summarize, the main two problems of an extraction section based on a quasi-periodic disk loaded structure are: 1) minimization of reflections from output end in order to avoid oscillation at high power levels and 2) tapering of the output section in order to avoid breakdown and compensate for the velocity decrease of the electrons. In order to optimize

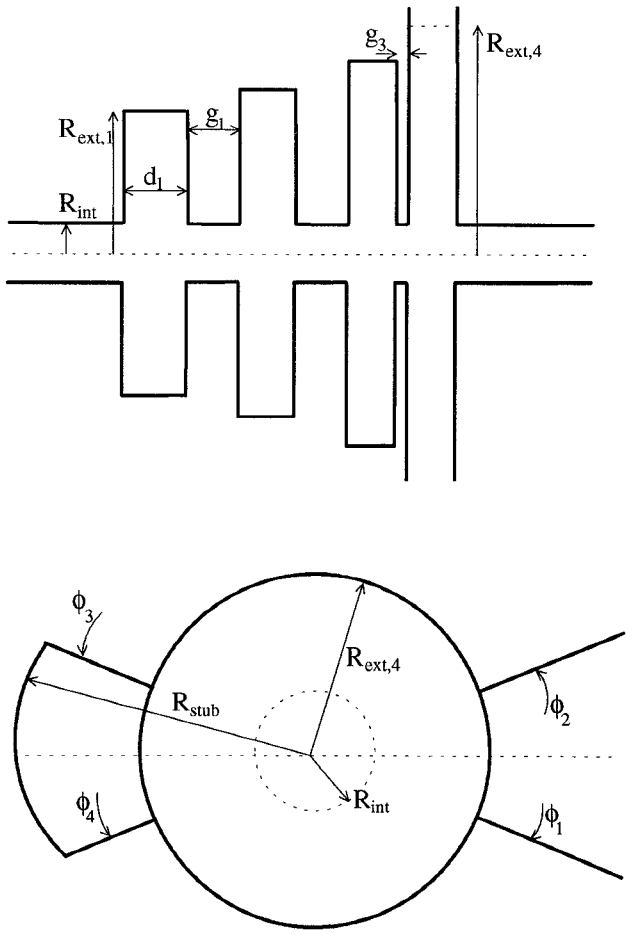

Fig. 1. The schematic of the system under consideration. The external radius $R_{\rm ext}$, the groove/arm width d and the separation between any two cavities can be arbitrary. The internal radius $R_{\rm int}$ has to be maintained the same. The asymmetry in the system is introduced by the output arm and the stub as illustrated.

these two conflicting requirements we have developed an analytical technique [8], [9] which permits design of a quasi-periodic structure. In Ref. 8 the pure electromagnetic problem is presented in the sense that an incident wave is injected into the structure and the effect of the various geometrical parameters on the transmission/reflection pattern are examined. The technique was further developed [9] to account for current sources or electron beams within the framework of the hydrodynamic model. In all these cases the system was assumed to be symmetrical, including the input and output arm.

In this study we present the analysis of a quasi-periodic structure and an *asymmetric* arm to account for a realistic coupling to a regular (rectangular) waveguide. In order to match the output arm to the quasi-periodic structure a tuning stub is attached to the output cavity. In literature [10], [11], there are two quasi-analytical methods for characterization of similar structures: the transmission matrix method and the scattering matrix method. The first method becomes unstable when many discontinuities have to be considered due to the very large or very small numbers associated with the evanescent waves which are necessary to retain in order to have an accurate information about the phase. Furthermore, it can not describe (without pure numerical methods) the coupling to symmetric input/output arms. The second method is more stable but to the best of our knowledge it is difficult in its framework to describe the beam wave interaction.

II. Green's Function

The quasi-periodic structure consists of a series of pill box like cavities attached to an "infinitely" long pipe of radius $R_{\rm int}$. Two radial arms are connected to the last cavity; one arm is open allowing wave propagation and the other is short circuited to model a stub tuner. The schematics of the system are presented in Fig. 1. In this particular study we have in mind the output section of a high power microwave structure which is fed by a bunched beam. Therefore we do not include an input arm. The width of each one of the cavities is denoted by $d_n, n = 1, 2 \cdots N$; where N is the total number of cavities. The cavities can be of any dimension provided that the basic geometry is preserved.

For a symmetric system the field in the inner cylinder ($0 < r < R_{\rm int}$) can be represented by the zero order azimuthal Floquet-harmonic. In the present system the two arms break the azimuthal symmetry therefore we have to consider the entire spatial spectrum of waves. In this region the electromagnetic field has two components: one which is the contribution of the current density in the absence of any boundaries—also called the primary field. The second contribution is a result of the metallic surface and the boundary conditions associated with their presence. This is also referred as the secondary field. However the current density which excites the primary field is taken to be azimuthally symmetric thus we shall consider only the symmetric contribution of the free space Green function. Subject to these conditions the magnetic vector potential in the pipe is given by

$$\begin{aligned} A_z(r,z,\phi;\omega) = {} & 2\pi\mu_0 \int_0^{R_b} dr'\, r' \\ & \cdot \int_{-\infty}^{\infty} dz'\, G_\omega(r,z|r',z') J_z(r',z';\omega) \\ & + \int_{-\infty}^{\infty} dk \sum_{m=-\infty}^{\infty} A_m(k) I_m(\Gamma r) \\ & \cdot e^{-\jmath kz} e^{-\jmath m\phi} \end{aligned} \tag{1}$$

where $\Gamma^2 = k^2 - \omega^2/c^2, I_m(x)$ is the mth order modified Bessel function of the first kind and the system is assumed to be in steady state ($e^{\jmath\omega t}$). The free space Green's function is given by

$$G_\omega(r,z|r',z') = \int_{-\infty}^{\infty} dk\, g_k(r|r') e^{-jk(z-z')} \tag{2}$$

and

$$\begin{aligned} g_k(r|r') = {} & \frac{1}{(2\pi)^2} \\ & \cdot \begin{cases} I_0(\Gamma r) K_0(\Gamma r') & 0 < r < r' < \infty \\ I_0(\Gamma r') K_0(\Gamma r) & 0 < r' < r < \infty. \end{cases} \end{aligned} \tag{3}$$

The first term in (1) is the magnetic vector potential associated with the primary field and from the second term one derives the secondary electromagnetic field. Note that

the other two components of the magnetic vector potential are zero ($A_r = 0$ and $A_\Phi = 0$) and the scalar electric potential is derived using the Lorentz gauge i.e. $\phi(r,z;\omega) = -(c^2/j\omega)(\partial A_z(r,z;\omega)/\partial z)$.

In the grooves the electromagnetic field can be represented by a superposition of modes which satisfy the boundary conditions on the metallic walls. In principle an infinite number of such modes should be taken. Our experience indicates that as long as the vacuum wavelength is about five times larger than the groove/arm width the first mode [transverse electric magnetic (TEM)] is sufficient for most practical purposes. This assumption is by no means critical for the present analysis and the arguments are very similar when a larger number of modes is required. However, we use it since it makes the presentation much simpler. In order to quantify this statement let us give a simple example of a periodic disk loaded structure: consider the case when R_{ext} = 15.9 mm, R_{int} = 9.0 mm, the period of the system is 10.0 mm and the disk is 5 mm wide. For this geometry it is required that the phase advance per cell will be 120° at 9 GHz. With 39 spatial (longitudinal) Floquet harmonics, the lower cutoff frequency ($kL = 0$), using three modes (TEM, TM_{01} and TM_{02}) in the grooves, was calculated to be 8.206 GHz, with two modes (TEM and TM_{01}) 8.192 GHz and 8.192 GHz when only the TEM mode was used. For the higher cutoff ($kL = \pi$) the calculated frequencies were 9.270, 9.229, and 9.229 GHz, correspondingly. Thus in the regime of interest the the typical error associated with the neglection of the higher modes in the grooves is expected to be on the order of 1% or less. According to the assumption above in each one of the grooves (with the exception of the last one) the magnetic vector potential is given by

$$A_z^n(r,z;\phi\omega) = \sum_{m=-\infty}^{\infty} D_n^{(m)} T_{m,n}\left(\frac{\omega}{c}r\right) e^{-jm\phi}, \tag{4}$$

where $D_n^{(m)}$ is the amplitude of the magnetic vector potential in the nth groove.

$$T_{m,n}\left(\frac{\omega}{c}r\right) = J_m\left(\frac{\omega}{c}r\right) Y_m\left(\frac{\omega}{c}R_{\text{ext},n}\right) - Y_m\left(\frac{\omega}{c}r\right) J_m\left(\frac{\omega}{c}R_{\text{ext},n}\right)$$

and $R_{\text{ext},n}$ is the external radius of the nth groove; later we shall also use the function

$$T'_{m,n}\left(\frac{\omega}{c}r\right) = J'_m\left(\frac{\omega}{c}r\right) Y_m\left(\frac{\omega}{c}R_{\text{ext},n}\right) - Y'_m\left(\frac{\omega}{c}r\right) J_m\left(\frac{\omega}{c}R_{\text{ext},n}\right).$$

The prime denotes the derivative with respect to the argument of the function. As above the other two components of the magnetic vector potential are zero and when considering only a single mode in the grooves the electric scalar potential is zero.

In the output cavity ($R_{\text{int}} < r < R_{\text{ext},N}$) there are two waves. One wave propagates outwards and is represented by mth order Hankel function of the second kind $H_m^{(2)}((\omega/c)r)$. The other wave is reflected by the external wall and propagates inwards thus is represented by $H_m^{(1)}((\omega/c)r)$. Hence:

$$A_z[R_{\text{int}} < r < R_{\text{ext},4}, \phi, |z - z(N)| < d(N)/2; \omega] = \sum_{m=-\infty}^{\infty} \left[U_m H_m^{(1)}\left(\frac{\omega}{c}r\right) + V_m H_m^{(2)}\left(\frac{\omega}{c}r\right)\right] e^{-jm\phi}. \tag{5}$$

This solution satisfies the boundary conditions at $r = R_{\text{ext},N}$. Consequently the two sets of amplitudes U_m and V_m are related by a reflection matrix

$$U_m = \sum_{m'=-\infty}^{\infty} R_{m,m'} V_{m'}. \tag{6}$$

In the next section we shall show how to determine this matrix. At the moment we shall consider it, as known. Next we define the functions

$$H_{m,m'}\left(\frac{\omega}{c}r\right) \equiv H_m^{(2)}\left(\frac{\omega}{c}r\right)\delta_{m,m'} + H_m^{(1)}\left(\frac{\omega}{c}r\right) R_{m,m'}$$

and

$$H'_{m,m'}\left(\frac{\omega}{c}r\right) \equiv H_m^{(2)\prime}\left(\frac{\omega}{c}r\right)\delta_{m,m'} + H_m^{(1)\prime}\left(\frac{\omega}{c}r\right) R_{m,m'}.$$

With the first function we can write (5) as

$$A_z[R_{\text{int}} < r < R_{ext,4}, \phi, |z - z(N)| < d(N)/2; \omega] = \sum_{m,m'=-\infty}^{\infty} H_{m.m'}\left(\frac{\omega}{c}r\right) V_{m'} e^{-jm\phi}. \tag{7}$$

As in the other grooves the other two components of the magnetic vector potential are zero and so is the electric scalar potential (subject the condition of a single longitudinal mode).

In order to determine the various amplitudes in terms of the known current density we impose next the boundary conditions at the only place where they are not satisfied as yet, $r = R_{\text{int}}$. The continuity of the longitudinal electric field (E_z) can be simplified to the form

$$A_m(k)I_m(\Delta) + B_m(k)K_m(\Delta) = -\frac{1}{2\pi}\frac{\alpha^2}{\Delta^2}\left[\sum_{n=1}^{N-1} D_n^{(m)} T_{m.n}(\alpha) d_n L_n(k) + d_N L_N(k) \sum_{m'=-\infty}^{\infty} H_{m,m'} V_{m'}\right] \tag{8}$$

whereas the continuity of the tangential magnetic field in the symmetric grooves

$$\alpha D_n^{(m)} T'_{m,n}(\alpha) = \int_{-\infty}^{\infty} dk L_n^*(k)\Delta[A_m(k)I'_m(\Delta) + B_m(k)K'_m(\Delta)]. \tag{9}$$

Similarly, in the output cell

$$\alpha \sum_{m'=-\infty}^{\infty} H'_{m,m'}(\alpha) V_{m'} = \int_{-\infty}^{\infty} dk\, L_N^*(k)\Delta[A_m(k)I'_m(\Delta) + B_m(k)K'_m(\Delta)]. \tag{10}$$

The following definitions have been used in the last expressions:

$$B_m(k) = \frac{1}{2\pi}\mu_0\delta_{m,0}\int_0^{R_b} dr' r' I_0(\Gamma r') \cdot \int_{-\infty}^{\infty} dz' e^{jkz'} J_z(r', z'; \omega), \tag{11}$$

$$L_n(k) = \frac{1}{d_n}\int_{z_n - d_n/2}^{z_n + d_n/2} dz e^{jkz}. \tag{12}$$

In addition $\delta_{m,n}$ is the Kroneker delta function, $\alpha = (\omega/c)R_{\text{int}}$ and $\Delta = \Gamma R_{\text{int}}$. As shown in [8], [9] it is convenient to substitute $A_m(k)$ from (8) in (9) and (10). The result reads

$$\sum_{n'=1}^{N-1}[T'_{m,n}(\alpha)\delta_{n,n'} + T_{m,n'}(\alpha)\chi^{(m)}_{n,n'}]D^{(m)}_{n'} + \chi^{(m)}_{n,N} \sum_{m'=-\infty}^{\infty} H'_{m,m'}(\alpha)V_{m'} = s^{(m)}_n \tag{13}$$

and

$$\sum_{m'=-\infty}^{\infty}[H'_{m,m'}(\alpha) + H_{m,m'}(\alpha)\chi^{(m)}_{N,N}]V_{m'} + \sum_{n=1}^{N-1} T_{m,n}(\alpha)\chi^{(m)}_{N,n}D^{(m)}_n = s^{(m)}_N. \tag{14}$$

In these expressions,

$$\chi^{(m)}_{n,n'} = \frac{d_{n'}\alpha}{2\pi}\int_{-\infty}^{\infty} dk \frac{I'_m(\Delta)}{\Delta I_m(\Delta)} L^*_n(k)L_{n'}(k) \tag{15}$$

and

$$s^{(m)}_n = -\frac{1}{\alpha}\int_{-\infty}^{\infty} dk B_m(k)\frac{1}{I_m(\Delta)}L^*_n(k). \tag{16}$$

In this study we do not consider the effect of the secondary electromagnetic field on the source i.e. electrons, therefore, the term $s^{(m)}_n$ is assumed to be given thus the formulation above permits us to calculate the amplitude in each one of the grooves. All the elements of the matrices involved are determined by analytic functions since, based on the Cauchy residue theorem, the χ matrix in (15) can be simplified to read

$$\chi^{(m)}_{n,n'} = \frac{\alpha}{R^2_{\text{int}}}\sum_{s=1}^{\infty}\begin{cases}\dfrac{2}{\Gamma^2_{s,m}}[1 - e^{-\Gamma_{s,m}d_n/2}\,\text{sinhc}\,(\Gamma_{s,m}d_n/2)] & n = n' \\ \dfrac{d'_n}{\Gamma_{s,m}} e^{-\Gamma_{s,m}|z_n - z'_n|}\,\text{sinhc}\,(\Gamma_{s,m}d_n/2) \cdot \text{sinhc}\,(\Gamma_s d_{n'}/2) & \text{otherwise}\end{cases} \tag{17}$$

where $\Gamma_{s,m} = \sqrt{(p_{s,m}/R_{\text{int}})^2 - (\omega/c)^2}$, $p_{s,m}$ is the sth zero of the Bessel function of the first kind of order m and $\text{sinhc}\,(x) \equiv \sinh(x)/x$.

III. Reflection Matrix

The coupling between the various azimuthal harmonics occurs in the last cell and in this section we shall formulate it in terms of a reflection matrix introduced in (6). In the last cell $[R_{\text{int}} < r < R_{\text{ext},n}, |z - z_N| < d_N/2$ and $0 < \phi < 2\pi]$ the magnetic vector potential is given by (5). In the stub this potential is given by

$$A_z[R_{\text{ext},N} < r < R_s, \phi_3 < \phi < \phi_4, |z - z(N)| < d(N)/2; \omega] = \sum_{m=1}^{\infty} S_m t_{\sigma(m)}\left(\frac{\omega}{c}r\right)\sin[\sigma(m)(\phi - \phi_3)] \tag{18}$$

where $\sigma(m) \equiv \pi m/(\phi_4 - \phi_3)$, R_{stub} is the external radius of the stub and

$$t_\sigma\left(\frac{\omega}{c}r\right) = J_\sigma\left(\frac{\omega}{c}r\right)Y_\sigma\left(\frac{\omega}{c}R_{\text{stub}}\right) - Y_\sigma\left(\frac{\omega}{c}r\right)J_\sigma\left(\frac{\omega}{c}R_{\text{stub}}\right).$$

We shall also use

$$t'_\sigma\left(\frac{\omega}{c}r\right) = J'_\sigma\left(\frac{\omega}{c}r\right)Y_\sigma\left(\frac{\omega}{c}R_{\text{stub}}\right) - Y'_\sigma\left(\frac{\omega}{c}r\right)J_\sigma\left(\frac{\omega}{c}R_{\text{stub}}\right).$$

In a very similar way, the magnetic vector potential in the output arm is given by

$$A_z[R_{\text{ext},N} < r < R_s, \phi_1 < \phi < \phi_2, |z - z(N)| < d(N)/2; \omega] = \sum_{m=1}^{\infty} D^{(m)}_N H^{(2)}_{\nu(m)}\left(\frac{\omega}{c}r\right)\sin[\nu(m)(\phi - \phi_1)] \tag{19}$$

with $\nu(m) = \pi m/(\phi_2 - \phi_1)$.

Imposing the continuity of the tangential components of the electromagnetic field at $r = R_{\text{ext},N}$ and after some algebraic manipulations we obtain

$$R_{m,m'} = -\sum_{n=-\infty}^{\infty}[\rho^{(1)}]^{-1}_{m,n}[\rho^{(2)}]_{n,m'} \tag{20}$$

where

$$\rho^{(i)}_{m,m'} = H^{(i)}_m(\xi)\delta_{m,m'} - \frac{\phi_2 - \phi_1}{\pi}H^{(i)\prime}_{m'}(\xi) \cdot \sum_{n=1}^{\infty}\frac{H^{(2)}_{\nu(n)}(\xi)}{H^{(2)\prime}_{\nu(n)}(\xi)}M_{m,n}(\phi_1;\phi_2)M^*_{m',n}(\phi_1;\phi_2) - \frac{\phi_4 - \phi_3}{\pi}H^{(i)\prime}_{m'}(\xi) \cdot \sum_{n=1}^{\infty}\frac{t_{\sigma(n)}(\xi)}{t'_{\sigma(n)}(\xi)}M_{m,n}(\phi_3;\phi_4)M^*_{m',n}(\phi_3;\phi_4), \tag{21}$$

$\xi = (\omega/c)R_{\text{ext},N}$ and

$$M_{m,n}(x_1;x_2) \equiv \frac{1}{x_1 - x_2}\int_{x_1}^{x_2} d\phi\, e^{jm\phi}\sin\left[\pi n\frac{\phi - x_1}{x_2 - x_1}\right]. \tag{22}$$

This concludes the formulation part of this study. In the next section we present one example of the use of this technique, with emphasis on the effect of the arm and the stub.

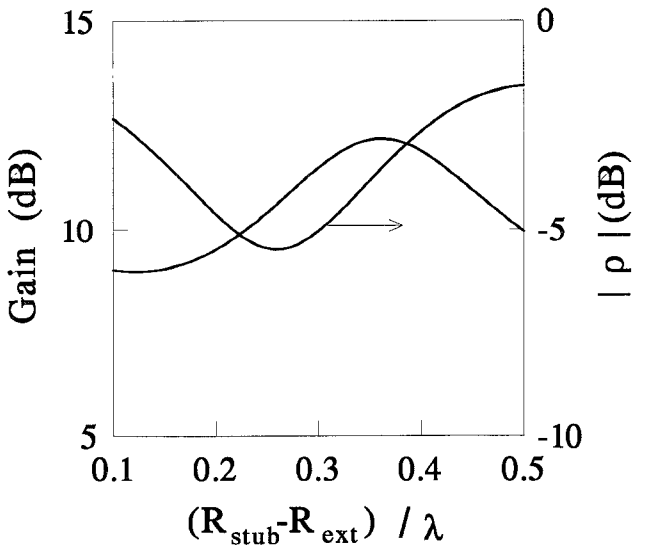

Fig. 2. The "gain" as defined in (28) and the reflection from the wall (in dB) of the zero azimuthal harmonic.

IV. Discussion and Conclusions

In order to illustrate the potential of the technique presented above, we consider a current distribution which models interaction in a traveling wave structure at the limit of saturation. It has the form

$$J_z(r,z;\omega) = J_0 e^{-jKz}\left(1-\frac{z}{d_{\rm sat}}\right)\theta(R_b-r) \qquad (23)$$

where the term $1-(z/d_{\rm sat})$ accounts for the saturation effect in a high efficiency system jh(x) is the heavyside step function. The characteristic saturation length $d_{\rm sat}$ is taken here to be 1.2 times larger than the total length of the system. The space-charge wavenumber K is assumed to be complex and has the form $K=(\omega/c)(1/\beta_{av})+\delta k(1+j\sqrt{3})$ as in a traveling wave tube at resonance; β_{av} is the normalized average velocity of the electrons at the input. The results presented below are for β_{av} = 0.94, δk = 60 m^{-1} and for a beam radius R_b = 2 mm.

It is convenient to normalize the amplitude of the magnetic vector potential with $J_0\pi R_b^2\mu_0$. Thus, the total power emitted in the presence of the structure (subscript $_{st}$) through the output arm is given by

$$\overline{P}_{st} \equiv \frac{P}{\frac{1}{2}(J_0\pi R_b^2)^2\eta_0} = \left(\frac{\omega}{c}d_N\right)\frac{\phi_2-\phi_1}{\pi}\sum_{n=1}^{\infty}|\overline{D}_N^{(n)}|^2, \qquad (24)$$

where $\overline{D}_N^{(n)} \equiv D_N^{(n)}/J_0\pi R_b^2\mu_0$. Now we introduce the numerical values of the geometrical parameters of the structure under consideration: the inner radius is $R_{\rm int}$ = 9 mm, the external radii of the cavities are $R_{ext,1\text{-}4}$ = 2.86, 3.00, 3.28 and 3.50 cm respectively; the widths $d_{1\text{-}4}$ = 4.4, 4.0, 3.6 and 5.0 mm. The drift region is 6 mm between the first three cavities and 1 mm between the third and fourth cavity. The output arm occupies the region between $-30°<\phi<30°$ and the stub between $150°<\phi<180°$. For the calculation of the reflection matrix 11 azimuthal harmonics ($-5<m<5$) and 18 radial modes were retained. Finally the operation frequency is 9 GHz.

TABLE I
Maximum Gain and Minimum Reflection for Various Span of the Stub or Arm; in Brackets the Stub Length ($R_{\rm stub}-R_{\rm ext,4}$)

	Arm. -18.0< ϕ <18.0	Arm -22 5< ϕ <22.5	Arm -30 0< ϕ <30 0
Stub 162 0< ϕ <198 0	|ρ| = -4 0dB (0 35λ) Gain = 11.4dB (0 46λ)	|ρ| = -4 2dB (0 35λ) Gain = 11 6dB (0 46λ)	|ρ| = -4 5dB (0 35λ) Gain = 12.2dB (0 46λ)
Stub 157 5< ϕ <202 5	|ρ| = -4 3dB (0 30λ) Gain = 11 5dB (0 41λ)	|ρ| = -4 4dB (0 30λ) Gain = 11 8dB (0 41λ)	|ρ| = -4 8dB (0 30λ) Gain = 12 3dB (0 41λ)
Stub 150 0< ϕ <210 0	|ρ| = -4 9dB (0.26λ) Gain = 11 3dB (0 36λ)	|ρ| = -5.1dB (0 26λ) Gain = 11 6dB (0.36λ)	|ρ| = -5 5dB (0 26λ) Gain = 12 2dB (0 36λ)

In order to emphasize the effect of the structure we shall compare the above power with the power emitted by the same current distribution, but limited to the region $0<z<d_t$, in free space (subscript $_{f.s.}$). The latter reads

$$\overline{P}_{f.s} \equiv \frac{P}{\frac{1}{2}(J_0\pi R_b^2)^2\eta_0} = \left(\frac{\omega}{c}d_t\right)^2\frac{1}{6\pi}g\left(d_{\rm sat},d_t,K,\frac{\omega}{c}\right), \qquad (25)$$

where

$$g\left(d_{\rm sat},d_t,K,\frac{\omega}{c}\right) \equiv \frac{3}{4}\int_0^{\pi}d\theta\sin^3\theta \cdot\left|F\left(\frac{d_t}{d_{\rm sat}},\xi=\frac{d_t}{2}\left(K-\frac{\omega}{c}\cos\theta\right)\right)\right|^2, \qquad (26)$$

d_t is the total length of the structure, and

$$F\left(\frac{d_t}{d_{\rm sat}},\xi\right) \equiv e^{-j\xi}\,\mathrm{sinc}(\xi) - j\frac{1}{2}\frac{d_t}{d_{\rm sat}}e^{-j\xi} \cdot\left[-j\,\mathrm{sinc}(\xi)+\frac{\xi\cos(\xi)-\sin(\xi)}{\xi^2}\right]. \qquad (27)$$

Based on the this quantity, we can define the gain as

$$\text{Gain (dB)} \equiv 10\log\left[\frac{\overline{P}_{st}}{\overline{P}_{f\,s.}}\right] \qquad (28)$$

which is illustrated in Fig. 2 as a function of the stub length. In addition we plotted on the same graph the effective reflection coefficient of the zero harmonics from $r=R_{\rm ext,4}$ i.e. $\rho=R_{0,0}$. There are two major factors which are apparent here: 1) the stub acts as a tuner and 2) the maximum gain does not occur for minimum reflection. We examined this feature for $2.0<R_{\rm ext,4}[\rm cm]<3.5$ and there was practically no change in the value of the maximum gain. However, the geometry of the stub has to be changed in order to achieve this maximum. The angular span of the stub and the arm have minor effect on the maximum gain and minimum reflection but a significant impact on the geometrical condition for their occurrence ($(R_{\rm stub}-R_{\rm ext,4})/\lambda$). This fact is summarized in Table I. Varying the angular span of the arm has a smaller

effect than changing that of the stub. Furthermore we found a small increase (1 dB) when the central axis of the stub was perpendicular (rather than anti-parallel) to that of the output arm.

REFERENCES

[1] G. A. Loew, "Review of studies on on conventional linear colliders in the S and X-band regime," in *Proc. HEACC'92, XV^{th} Int Conf. High Energy Accelerators,* 1992, p. 777.

[2] D. A. Shiffler, J. A. Nation, J. D. Ivers, G. S. Kerslick, and L. Schächter, "A Two stage high power traveling wave tube amplifier," *Appl. Phys. Lett.*, vol. 58, p. 899, 1991.

[3] ——, "A high power two stage traveling wave Tube amplifier," *J. Appl. Phys.*, vol. 70, no. 1 p. 106, 1991.

[4] L. Schächter, J. A. Nation, and D. A. Shiffler, "Theoretical studies of high power Cerenkov amplifiers," *J. Appl. Phys.*, vol. 70, no. 1, pp. 114–124, 1991.

[5] L. Schächter and J. A. Nation, "Slow wave amplifiers and oscillators: A unified study," *Phys. Rev. A*, vol. 45, pp. 8820–8832, 1992.

[6] L. Schächter and J. A. Nation, "Narrow band high power traveling wave amplifier," *The Third Workshop on Advanced Acceleration Concepts*, Port Jefferson, Long Island, NY, pp. 14–20, June 1992.

[7] E. Kuang, T. J. Davis, G. S. Kerslick, J. A. Nation, and L. Schächter, "Transient time isolation of a traveling wave amplifier," in *Phys. Rev. Lett.*

[8] L. Schächter and J. A. Nation, "An analytical method for studying quasiperiodic disk loaded waveguide," *Appl. Phys. Lett.*, vol. 63, no. 17, pp. 1–3, 1993.

[9] L. Schächter and J. A. Nation, "An analytical approach for analysis and design of quasiperiodic structure for high power microwave sources," private communication.

[10] L. Lewin, *Theory of Waveguides.* New York-Toronto: John Wiley & Sons, 1970.

[11] R. Mittra and S. W. Lee, *Analytical Techniques in the Theory of Guided Waves.* New York: Macmillan, 1971.

Levi Schächter, photograph and biography not available at the time of publication.

John A. Nation, photograph and biography not available at the time of publication.